

Stick Graphs with Length Constraints^{*}

Steven Chaplick¹, Philipp Kindermann¹, Andre Löffler¹, Florian Thiele¹,
Alexander Wolff¹, Alexander Zaft¹, and Johannes Zink¹

Institut für Informatik, Universität Würzburg
firstname.lastname@uni-wuerzburg.de

Abstract. Stick graphs are intersection graphs of horizontal and vertical line segments that all touch a line of slope -1 and lie above this line. De Luca et al. [GD'18] considered the recognition problem of stick graphs for the case that the order of either one of the two sets (STICK_A) is given and for the case that the order of both sets is given (STICK_{AB}). They showed how to solve both cases efficiently. In this paper, we improve the running times of their algorithms and consider new variants of STICK , where no order is given, STICK_A , and STICK_{AB} where the lengths of the sticks are given as input. We show that all new problem variants are NP-complete and give an efficient solution for STICK_{AB} with fixed stick lengths if there are no isolated vertices.

1 Introduction

For a given collection \mathcal{S} of geometric objects, the *intersection graph* of \mathcal{S} has \mathcal{S} as its vertex set and an edge whenever $S \cap S' \neq \emptyset$, for $S, S' \in \mathcal{S}$. This paper concerns *recognition* problems for classes of intersection graphs of restricted geometric objects, i.e., determining whether a given graph is an intersection graph of a family of restricted sets of geometric objects. A classic (general) class of intersection graphs is that of *segment graphs*, the intersection graphs of line segments in the plane¹. For example, segment graphs are known to include planar graphs [4]. The recognition problem for segment graphs is $\exists\mathbb{R}$ -complete [16,20]². On the other hand, one of the simplest natural subclasses of segment graphs is that of the *permutation* graphs, which are the intersection graphs of line segments where there are two parallel lines such that each line segment has its two end points on these parallel lines³, we say that the segments are *grounded* on these two lines. The recognition problem for permutation graphs can be solved in linear time [17]. *Bipartite* permutation graphs have an even simpler intersection representation [23]: they are the intersection graphs of unit-length

^{*} S.C. and A.W. acknowledge support from DFG grants WO 758/11-1 and WO 758/9-1.

¹ We follow the common convention that parallel segments do not intersect and each point in the plane belongs to at most two segments.

² Note that $\exists\mathbb{R}$ includes NP, see [20,22] for background on the complexity class $\exists\mathbb{R}$.

³ i.e., we think of the sequence of end points on the “bottom” line as one permutation π on the vertices and the sequence on the top line as another permutation π' , where uv is an edge if and only if the order of u and v differs in π and π' .

vertical and horizontal line segments which are again double-grounded (without loss of generality both lines have a slope of -1). The simpler structure of bipartite permutation graphs leads to a simpler linear-time recognition algorithm [25] than that of permutation graphs.

Several recent articles [1,2,6,7] compare and study the geometric intersection graph classes occurring between the simple classes, such as bipartite permutation graphs, and the general classes, such as segment graphs. Cabello and Jejčič [1] mention that studying such classes with constraints on the sizes or lengths of the objects is an interesting direction for future work (and such constraints are the focus of our work). Note that similar length restrictions have been considered for other geometric intersection graphs such as interval graphs [13,14,21].

When the segments are not grounded, but still are only horizontal and vertical, the class is referred to as *grid intersection graphs* and it also has a rich history, see, e.g., [6,7,11,15]. In particular, note that the recognition problem is NP-complete for grid intersection graphs [15]. But, if both the permutation of the vertical segments and the permutation of the horizontal segments are given, then the problem becomes a trivial check on the bipartite adjacency matrix [15]. However, for the variant where only one such permutation, e.g., the order of the horizontal segments, is given, the complexity remains open. A few special cases of this problem have been solved efficiently [5,19,8], e.g., one such case [5] is equivalent to the problem of *level planarity testing* which can be solved in linear time [12].

In this paper we study recognition problems concerning so-called *stick graphs*, the intersection graphs of grounded vertical and horizontal line segments (i.e., grounded grid intersection graphs). Classes closely related to stick graphs appear in several application contexts, e.g., in *nano PLA-design* [24] and detecting *loss of heterozygosity events in the human genome* [3,10]. Note that, similar to the general case of segment graphs, it was recently shown that the recognition problem for grounded segments (where arbitrary slopes are allowed) is $\exists\mathbb{R}$ -complete [2]. So, it seems likely that the recognition problem for stick graphs is NP-complete (similar to grid intersection graphs), but thus far it remains open. The primary prior work on recognizing stick graphs is due to De Luca et al. [19]. Similarly to Kratochvíl's approach to grid intersection graphs [15], De Luca et al. characterized stick graphs through their bipartite adjacency matrix and used this result as a basis to develop polynomial-time algorithms to solve two constrained cases of the stick graph recognition problem called STICK_A and STICK_{AB} , defined next.

Definition 1 (STICK). *Let G be a bipartite graph with vertex set $A \dot{\cup} B$. The task is to decide whether G has a stick representation where the vertices in A are vertical segments and the vertices in B as horizontal segments on a ground line of slope -1 . We call such a realization a stick realization of G , and we call the line segments in a realization sticks.*

Definition 2 ($\text{STICK}_A/\text{STICK}_{AB}$). *In the problem STICK_A (STICK_{AB}) we are given an instance of the STICK problem and additionally an order σ_A (orders σ_A, σ_B) of the vertices in A (in A and B). The task is to decide whether there is a stick realization that respects σ_A (σ_A and σ_B).*

Table 1: Previously known and new results for deciding whether a given bipartite graph $G = (A \dot{\cup} B, E)$ is a stick graph. In $O(\cdot)$, we dropped $|\cdot|$. NPC means NP-complete.

given order	variable length				fixed length			
	old		new		isolated vertices		no isolated vertices	
\emptyset	unknown		unknown		NPC	Thm. 3	NPC	Thm. 3
A	$O(A^3 B^3)$	[19]	$O(AB)$	Thm. 1	NPC	Thm. 4	NPC	Thm. 4
A, B	$O(AB)$	[19]	$O(E)$	Thm. 2	NPC	Cor. 2	$O((A+B)^2)$	Cor. 3

Our Contribution. We first revisit the problems STICK_A and STICK_{AB} defined by De Luca et al. [19] and provide faster algorithms for them; see Section 2. Their and our new results are listed in Table 1 (NPC stands for NP-complete). Then we investigate the direction suggested by Cabello and Jeřčič [1] where specific lengths are given for the segments of each vertex. In particular, this can be thought of as generalizing from unit stick graphs (i.e., bipartite permutation graphs), where every segment has the same length. While bipartite permutation graphs can be recognized in linear time [25], it turns out that all of the new problem variants (which we call $\text{STICK}^{\text{fix}}$, $\text{STICK}_A^{\text{fix}}$, and $\text{STICK}_{AB}^{\text{fix}}$) are NP-complete; see Section 3. Finally, we give an efficient solution for $\text{STICK}_{AB}^{\text{fix}}$ (that is, STICK_{AB} with fixed stick lengths) for the special case that there are no isolated vertices (see Section 3.3). We conclude and state some open problems in Section 4.

2 Sticks of Variable Lengths

In this section, we provide algorithms for the STICK_A problem in $O(|A||B|)$ time (Theorem 1) and the STICK_{AB} problem in $O(|A| + |B| + |E|)$ time (Theorem 2).

Theorem 1. *STICK_A can be solved in $O(|A||B|)$ time.*

Proof. (Here we assume that G is connected and discuss otherwise in Appendix A). To prove this, we apply a sweep-line approach (with a vertical sweep-line that moves rightwards) where each vertical stick v_i corresponds to two events: the *enter event* of v_i (abbreviated by $i \mapsto$) and the *exit event* of v_i (abbreviated by $i \mapsto$). During the sweep, we maintain a data structure that compactly encodes all *realizable* permutations for the horizontal sticks that *must* pass through the current position of the sweep line (as restricted by vertical sticks on or left of the current position) as to proceed with the next event. For each event $p \in \{i \mapsto, i \mapsto\}$, we denote the data structure by \mathcal{T}^p , the sticks of B in \mathcal{T}^p by B^p , and by G^p the induced subgraph of G containing v_1, \dots, v_i and their neighbors.

In the enter event of v_i , we add to the data structure all the vertices of B that neighbor v_i and aren't in the data structure yet (we call these *entering vertices*), and constrain the data structure so that all the neighbors of v_i must occur after (below) the non-neighbors of v_i . In the *exit event* $i \mapsto$, we remove from the data structure all sticks of B that do not have any neighbor v_j with $j > i$, i.e., they

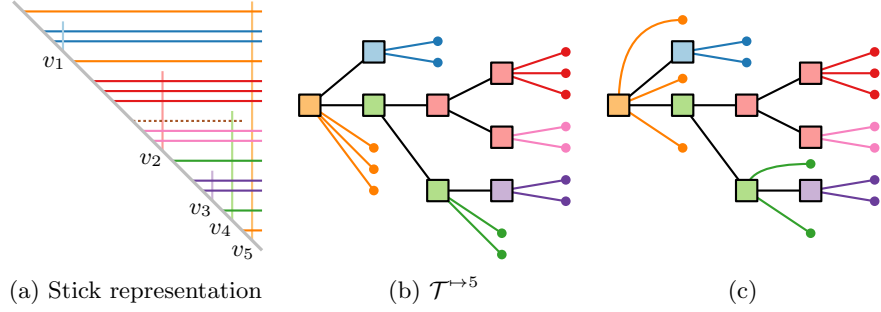


Fig. 1: An example for $\mathcal{T}^{i \mapsto 5}$. The dotted stick has left the data structure. In (c), the leaves are permuted among the children to match the representation.

have v_i as their last neighbor (we call these *leaving vertices*). Hence, each $B^{i \mapsto i}$ ($B^{i \mapsto}$) consists of all sticks of B with a neighbor in v_1, \dots, v_i (v_1, \dots, v_i) and a neighbor in $v_i, \dots, v_{|A|}$ ($v_{i+1}, \dots, v_{|A|}$),

We can now discuss our data structure; see Fig. 1 for an example. Consider any event p . Observe that G^p may consist of several components $G_1^p, \dots, G_{k_p}^p$. The components are naturally ordered from left to right by σ_A . Let B_j^p denote the vertices of B^p in G_j^p . In this case, in every realizable permutation of B^p , the vertices of B_j^p must come before the vertices of B_{j+1}^p . Furthermore, the vertices that will be introduced any time later can only be placed in the beginning, end, or between the components. Hence, to compactly encode the realizable permutations, it suffices to do so for each component G_j^p individually via a data structure T_j^p . Namely, our data structure will be $\mathcal{T}^p = (T_1^p, \dots, T_{k_p}^p)$.

Each data structure T_j^p is a rooted tree. It expresses the realizable permutations of B_j^p . At each node, its children consist of two types: the leaves (which correspond to the vertices of B_j^p) and the non-leaves. The non-leaves are ordered, while the leaves are unordered and can be placed anywhere before, after, or between the non-leaves with the same parent.

We will argue that this data structure is sufficient to express T_j^p by induction. In the base case, consider the enter event of v_i . Our data structure consists of a single component $G_1^{i \mapsto 1}$ and clearly a single node with a leaf-child for every neighbor of v_1 captures all possible permutations.

Consider the exit event of v_i and assume that after the enter event of i we have the data structure $\mathcal{T}^{i \mapsto i} = (T_1^{i \mapsto i}, \dots, T_k^{i \mapsto i})$. If there are no leaving vertices, we just keep the data structures and we are done. Otherwise, $B^{i \mapsto}$ is a strict subset of $B^{i \mapsto i}$. We delete all leaves from $\mathcal{T}^{i \mapsto i}$ corresponding to leaving vertices. If this results in any internal node having only one child and that child is an internal node, then we merge it with its parent. If all children of an internal node get removed, then we also remove the node. Obviously, this procedure maintains all realizable permutations of $B^{i \mapsto}$ due to $G^{i \mapsto}$.

Now, consider the enter event of v_i and assume that after the exit event of v_{i-1} we have the data structure $\mathcal{T}^{(i-1) \mapsto} = (T_1^{(i-1) \mapsto}, \dots, T_k^{(i-1) \mapsto})$. The essential

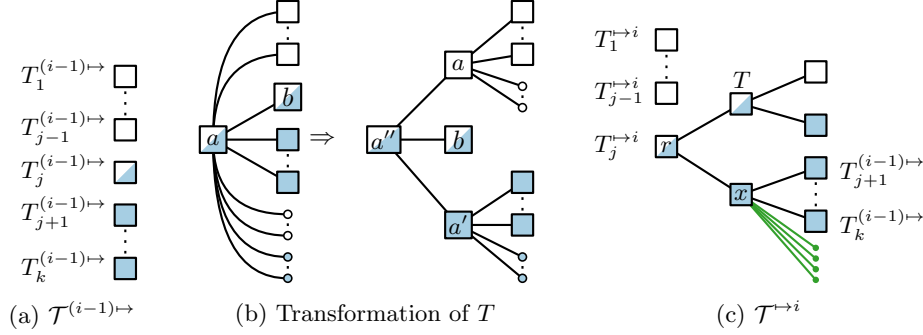


Fig. 2: Construction of $\mathcal{T}^{i \rightarrow i}$. The leaves at x are the entering vertices.

observation is that the neighbors of v_i must form a suffix in every realizable permutation after the enter event. Namely, either all vertices in $B^{(i-1) \mapsto}$ are adjacent to v_i , none of them are adjacent to v_i , or there is a j such that (i) $B_j^{(i-1) \mapsto}$ contains at least one neighbor of v_i ; (ii) all vertices in $B_{j+1}^{(i-1) \mapsto}, \dots, B_k^{(i-1) \mapsto}$ are neighbors of v_i ; and (iii) no vertices in $B_1^{(i-1) \mapsto}, \dots, B_{j-1}^{(i-1) \mapsto}$ are adjacent to v_i . Otherwise, there are no realizable permutations for this event and subsequently for G . The first two cases can be seen as degenerate cases (with $j = 0$ or $j = k + 1$) of the general case below; see Fig. 2a.

We first show how to process $T_j^{(i-1) \mapsto}$; see Fig. 2b. We create a tree T whose realizable permutations are precisely the subset of those of $T_j^{(i-1) \mapsto}$ where all leaves that are neighbors of v_i occur as a suffix. We initialize $T = T_j^{(i-1) \mapsto}$. If all vertices in $B_j^{(i-1) \mapsto}$ are neighbors of v_i , then we are already done.

Otherwise, we define a *marked* node as one where all leaves in its induced subtree are neighbors of v_i ; an *unmarked* node as one where no leaf in its induced subtree is a neighbor of v_i ; and a node is *half-marked* otherwise. Note that the root is half-marked. Since the neighbors of v_i must form a suffix, the marked non-leaf children of a half-marked node form a suffix, the unmarked non-leaf children form a prefix, and there is at most one half-mark child. Hence, the half-marked nodes form a path in T that starts in the root; otherwise, there are no realizable permutations for this event and subsequently for G .

We traverse the path bottom-up. Let a be a half-marked node, and let b be its half-marked child (if it exists). We create a new vertex a' and move all marked children of a to a' , preserving the order among the non-leaf children. Then we create a new node a'' and we hang a, b , and a' from a'' in this order. Finally, we put a'' into the former position of a in T . If this results in any internal node x with no leaf-children and only one child, we merge x with its parent. This ensures that all permutations realized by T have the neighbors of v_i as a suffix. Further, observe that the relation between two marked (or two unmarked) nodes is the same in T as in $T_j^{(i-1) \mapsto}$. The marked (unmarked) leaf-children of any

half-marked node a of $T_j^{(i-1) \mapsto}$ can be placed anywhere before, between, or after its marked (unmarked) children, but not before (after) b , since b has both marked and unmarked children. Hence, the permutations realized by T are exactly those realized by $T_j^{(i-1) \mapsto}$ that have the neighbors of v_i as a suffix.

Now, we create the data structure $\mathcal{T}^{\mapsto i}$; see Fig. 2c. We first set $T_1^{\mapsto i} = T_1^{(i-1) \mapsto}, \dots, T_{j-1}^{\mapsto i} = T_{j-1}^{(i-1) \mapsto}$. We additionally create $T_j^{\mapsto i}$ as follows. We hang $T_{j+1}^{(i-1) \mapsto}, \dots, T_k^{(i-1) \mapsto}$ from a new node x in this order. We further insert the entering vertices as leaf-children of x (note that this allows them to mix freely before, after, or between the components $G_{j+1}^{(i-1) \mapsto}, \dots, G_k^{(i-1) \mapsto}$). Then, we hang T followed by x off another node r , and make r the root of $T_j^{\mapsto i}$. Finally, we set $\mathcal{T}^{\mapsto i} = (T_1^{\mapsto i}, \dots, T_j^{\mapsto i})$. This way, the order of the components $G_1^{(i-1) \mapsto}, \dots, G_k^{(i-1) \mapsto}$ of $G^{(i-1) \mapsto}$ is maintained in the data structures for $G^{\mapsto i}$. Furthermore, we ensure that the entering vertices can be placed exactly before, after, or between the components of $G^{(i-1) \mapsto}$ that are completely adjacent to v_i . Hence, this data structure captures all realizable permutations of $B^{\mapsto i}$ due to $G^{\mapsto i}$.

The decision problem of **STICK_A** can be easily be solved by this algorithm. To find a realization, however, one has to backtrack through the data structures to find a valid permutation for the input problem. In Appendix A, we will show how to do the backtracking and that the whole algorithm takes $O(|A||B|)$ time. \square

Theorem 2. *STICK_{AB} can be solved in $O(|A| + |B| + |E|)$ time.*

Proof. We use the same enter and exit events as in the algorithm for **STICK_A**. However, the information that we maintain is simpler, and we also obtain a drawing directly. Let $\sigma_A = (a_1, \dots, a_{|A|})$ and $\sigma_B = (b_1, \dots, b_{|B|})$. Let β_i denote the largest index such that a_i is adjacent to b_{β_i} . Let $\hat{B}^{\mapsto i}$ be the elements of $(b_1, \dots, b_{\beta_i})$ that have a neighbor in $a_i, \dots, a_{|A|}$ ordered by σ_B , and let $\hat{B}^{i \mapsto}$ be the elements of $(b_1, \dots, b_{\beta_i})$ that have a neighbor in $a_{i+1}, \dots, a_{|A|}$. At every event $p \in \{\mapsto i, i \mapsto\}$, we maintain the invariants that (i) we have a valid representation of the subgraph of G induced by $b_1, \dots, b_{\beta_i}, a_1, \dots, a_i$; (ii) for each such vertex, its coordinate on the ground line is set, and these coordinates are the consecutive integers from 1 to $\beta_i + i$; and (iii) for those not in \hat{B}^p , their lengths are set.

Consider the enter event of a_i . We place v_i at position $\beta_i + i$. We place the vertices $b_{\beta_{i-1}+1}, \dots, b_{\beta_i}$ (if they exist) between v_{i-1} and v_i in this order and create $\hat{B}^{\mapsto i}$ by appending them to $\hat{B}^{(i-1) \mapsto}$ in this order. All neighbors of v_i have to be before v_i , and they have to be a suffix of $\hat{B}^{\mapsto i}$. This is easily checked in $\deg(v_i)$ time. The end point of v_i is placed directly above the foot point of its first neighbor in this suffix. As such, the invariants (i)–(iii) are maintained.

Consider the exit event of a_i and each neighbor b_j of a_i . If a_i is the last neighbor of b_j in σ_A , then we end b_j and set its endpoint at $\beta_i + i + 1/2$. We create $\hat{B}^{i \mapsto}$ by removing each such b_j from $\hat{B}^{\mapsto i}$. This again maintains invariants (i)–(iii). Hence, if we complete the exit event of $a_{|A|}$, we obtain a **STICK_{AB}** representation of G . Otherwise, G has no such representation. Clearly, the whole algorithm works in $O(|A| + |B| + |E|)$ time. Note that, even though we have not explicitly discussed isolated vertices, these are easily handled with length 0. \square

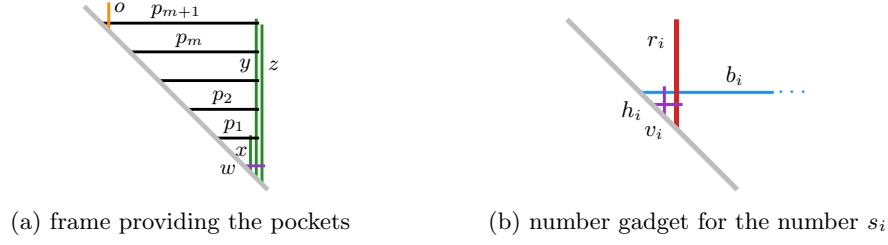


Fig. 3: Gadgets of our reduction from 3-PARTITION to $\text{STICK}^{\text{fix}}$.

3 Sticks of Fixed Lengths

In this section, we consider the case that, for each vertex of the input graph, its stick length is part of the input and fixed. We denote the variants of this problem by $\text{STICK}^{\text{fix}}$, by $\text{STICK}_A^{\text{fix}}$ if additionally σ_A is given, and by $\text{STICK}_{AB}^{\text{fix}}$ if σ_A and σ_B are given. Unlike the case with variable stick length, all three variants are NP-hard; see Sections 3.1 and 3.2. Surprisingly, $\text{STICK}_{AB}^{\text{fix}}$ can be solved efficiently by a simple linear program if the input graph contains no isolated vertices (i.e., vertices of degree 0); see Section 3.3. With our linear program, we can check the feasibility of any instance of $\text{STICK}^{\text{fix}}$ if we are given a total order of the sticks on the ground line. With our NP-hardness results, this implies NP-completeness.

3.1 $\text{STICK}^{\text{fix}}$

We show that $\text{STICK}^{\text{fix}}$ is NP-hard by reduction from 3-PARTITION, which is strongly NP-complete [9]. In 3-PARTITION, one is given a multiset S of $3m$ integers s_1, \dots, s_{3m} such that, for $i \in \{1, \dots, 3m\}$, $C/4 < s_i < C/2$, where $C = (\sum_{i=1}^{3m} s_i)/m$, and the task is to decide whether S can be split into m sets of three integers, each summing up to C .

Theorem 3. *$\text{STICK}^{\text{fix}}$ is NP-complete.*

Proof. We describe a polynomial-time reduction from 3-PARTITION. Given a 3-PARTITION instance $I = (S, C, m)$, we construct a fixed cage-like frame structure and introduce a number gadget for each number of S . A sketch of the frame is given in Fig. 3a. The purpose of the frame is to provide pockets, which will host our number gadgets (defined below). We add two long vertical (green) sticks y and z of length $mC + 1 + 2\varepsilon$ and a shorter vertical (green) stick x of length 1 that are all kept together by a short horizontal (violet) stick w of some length $\varepsilon \ll 1$. We use $m + 1$ horizontal (black) sticks p_1, p_2, \dots, p_{m+1} to separate the pockets. Each of them intersects y but not z and has a specific length such that the distance between two of these sticks is $C \pm \varepsilon$. Additionally, p_1 intersects x and p_{m+1} intersects a vertical (orange) stick o of length $2C$. We use x and o to prevent the number gadgets from being placed below the bottommost and above the topmost pocket, respectively. It does not matter on which side of y the stick x ends up since each b_i of a number gadget intersects y but neither x nor z .

For each number s_i in S , we construct a number gadget; see Fig. 3b. We introduce a vertical (red) stick r_i of length s_i . Intersecting r_i , we add a horizontal (blue) stick b_i of length at least $mC + 2$. The stick b_i intersects y and z , but neither x nor o . Due to these adjacencies, every number gadget can only be placed in one of the m pockets defined by p_1, \dots, p_{m+1} . It cannot span multiple pockets. We require that r_i and b_i intersect each other close to their foot points, so we introduce two short (violet) sticks h_i and v_i —one horizontal, the other vertical—of lengths ε ; they intersect each other, h_i intersects r_i , and v_i intersects b_i .

Given a yes-instance $I = (S, C, m)$ and a valid 3-partition P of S , the graph obtained by our reduction is realizable. Construct the frame as described before and place the number gadgets into the pockets according to P . Since the lengths of the three number gadgets' r_i sum up to $C \pm 3\varepsilon$, all three can be placed into one pocket. After distributing all number gadgets, we have a stick realization.

Given a stick realization of a graph G obtained from our reduction, we can obtain a valid solution of the corresponding 3-PARTITION instance $I = (S, C, m)$ as follows. Clearly, the shape of the frame is fixed, creating m pockets. Since the sticks b_1, \dots, b_{3m} are incident to y and z but neither to x nor to o , they can end up inside any of the pockets. In the y -dimension, each two number gadgets of numbers s_k and s_ℓ overlap at most on a section of length ε ; otherwise r_k and b_ℓ or r_ℓ and b_k would intersect. Each pocket hosts precisely three number gadgets: we have $3m$ number gadgets, m pockets, and no pocket can contain four (or more) number gadgets; otherwise, there would be a number gadget of height at most $(C + \varepsilon)/4 + 2\varepsilon$, contradicting the fact that s_i is an integer with $s_i > C/4$. In each pocket, the height of the number gadgets would be too large if the three corresponding numbers of S would sum up to $C + 1$ or more. Thus, the assignment of number gadgets to pockets defines a valid 3-partition of S . \square

The sticks of lengths s_1, \dots, s_{3m} can be simulated by paths of sticks with length ε each. Exploiting this, we can modify our reduction to use only three distinct stick lengths. We prove the following corollary in Appendix B.

Corollary 1. *$STICK^{\text{fix}}$ with only three different stick lengths is NP-complete.*

3.2 $STICK_A^{\text{fix}}$ and $STICK_{AB}^{\text{fix}}$

We show that $STICK_A^{\text{fix}}$ and $STICK_{AB}^{\text{fix}}$ are NP-hard by reduction from MONOTONE-3-SAT, which is NP-complete [18]. In MONOTONE-3-SAT, one is given a Boolean formula Φ in conjunctive normal form where each clause contains three distinct literals that are all positive or all negative. The task is to decide if Φ is satisfiable.

Theorem 4. *$STICK_A^{\text{fix}}$ is NP-complete.*

Proof. We describe a polynomial-time reduction from MONOTONE-3-SAT. A schematization of our reduction is depicted in Figs. 4 to 6. Given a MONOTONE-3-SAT instance Φ over variables x_1, \dots, x_n , we construct for each variable x_i (with $i \in \{1, \dots, n\}$) a *variable gadget* as depicted in Fig. 4. Inside a (black) *cage*, there is a vertical (red) stick r_i with length 1 and from inside, a long horizontal

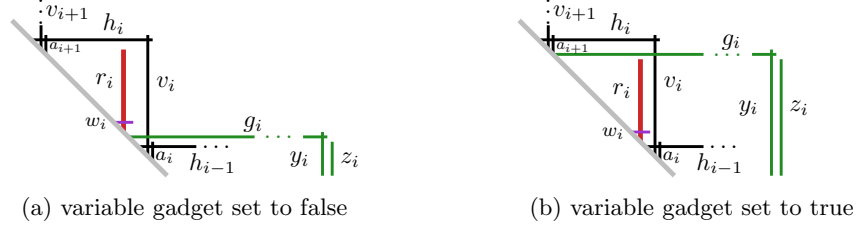


Fig. 4: Variable gadget in our reduction from MONOTONE-3-SAT to $\text{STICK}_A^{\text{fix}}$.

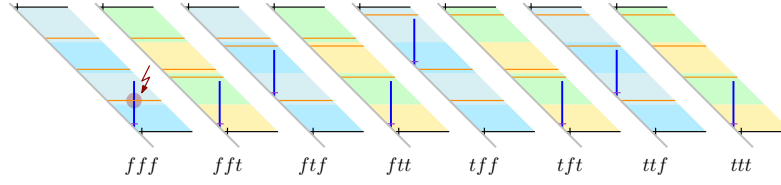


Fig. 5: Positive clause gadget (empty sub-stripe at the bottom). Here, a clause gadget for each of the eight possible truth assignments of a MONOTONE-3-SAT clause is depicted. E.g., tft means that the first variable is set to true, the second to false, and the third to true. Similarly, a negative clause gadget has an empty sub-stripe at the top.

(green) stick g_i leaves this cage. We can enforce the structure to look like in Fig. 4 as follows. We prescribe the order σ_A of the vertical sticks as in Fig. 4. Since a_{i+1} has length $\varepsilon \ll 1$, the horizontal (black) stick h_i intersects the two vertical (black) sticks v_{i+1} and a_{i+1} close to its foot point. We have $\sigma_A(a_{i+1}) < \sigma_A(r_i) < \sigma_A(v_i)$, so r_i is inside the cage bounded by h_i and v_i and fixed its height—as it does not intersect h_i —making sticks h_i and v_i intersect close to their end points (both have length $1 + 2\varepsilon$). Moreover, r_i cannot be below h_{i-1} because a_i is shorter than r_i and intersects h_{i-1} to the right of r_i . The stick w_i intersects r_i close to r_i 's foot point because w_i has length ε . This leaves the freedom of placing g_i above or below r_i (as g_i does not intersect r_i) but still with its foot point inside the cage formed by h_i and v_i because it intersects v_i , but neither v_{i-1} nor v_{i+1} .

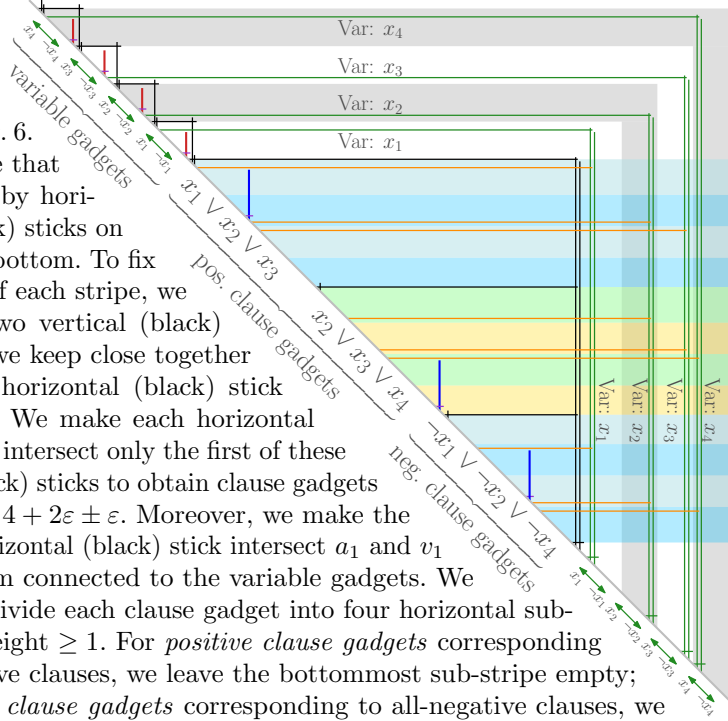
We say that the variable x_i is set to false if the foot point of g_i is below the foot point of r_i , and true otherwise. For each x_i , we add two long vertical (green) sticks y_i and z_i that we keep close together by a short horizontal (violet) stick of length ε (see Fig. 6 on the bottom right). We make g_i intersect y_i but not z_i . The three sticks g_i , y_i , and z_i get the same length ℓ_i . Hence, y_i and g_i intersect each other close to their end points as otherwise g_i would intersect z_i . We choose ℓ_1 sufficiently large such that the foot point of y_1 is to the right of the clause gadgets (see Fig. 6) and for each ℓ_i with $i \geq 2$, we set $\ell_i = \ell_{i-1} + 1 + 3\varepsilon$. Now compare the end points of g_i when x_i is set to false and when x_i is set to true relative to the (black) cage structure. When x_i is set to true, the end point of g_i is $1 \pm 2\varepsilon$ above and $1 \pm 2\varepsilon$ to the left compared to the case when x_i is set to false. Observe that, since g_i and y_i intersect each other close to their end points, this offset is also pushed to y_i and z_i and their foot points. Consequently, the

position of the foot point of y_i (and z_i) differs by $1 \pm 2\varepsilon$ relative to the (black) frame structure depending on whether x_i is set to true or false. Our choice of ℓ_i allows this movement. In other words, no matter which truth value we assign to each x_i , there is a realization of the variable gadgets respecting σ_A .

Fig. 6: Illustration of our reduction from MONOTONE-3-SAT to $\text{STICK}_A^{\text{fix}}$

For each clause, we add a *clause gadget* (see Fig. 5) as shown in Fig. 6. It is a stripe that is bounded by horizontal (black) sticks on its top and bottom. To fix the height of each stripe, we introduce two vertical (black) sticks that we keep close together by a short horizontal (black) stick of length ε . We make each horizontal (black) stick intersect only the first of these vertical (black) sticks to obtain clause gadgets of height of $4 + 2\varepsilon \pm \varepsilon$. Moreover, we make the topmost horizontal (black) stick intersect a_1 and v_1 to keep them connected to the variable gadgets. We (virtually) divide each clause gadget into four horizontal sub-stripes of height ≥ 1 . For *positive clause gadgets* corresponding to all-positive clauses, we leave the bottommost sub-stripe empty; for *negative clause gadgets* corresponding to all-negative clauses, we leave the topmost sub-stripe empty. We add three horizontal (orange) sticks—one per remaining horizontal sub-stripe—and assign them bijectively to the variables of the clause. We make each horizontal (orange) stick o that is assigned to x_i intersect y_i and all y_j and z_j for $j < i$, but not z_i or y_k or z_k for any $k > i$. Thus, o intersects y_i close to o_i 's end points. We choose the length of each such o so that its foot point is at the bottom of its sub-stripe if x_i is set to false or is at the top of its sub-stripe if x_i is set to true. Within the positive and the negative clause gadgets, this gives us two times eight possible configurations of the orange sticks depending on the truth assignment of the three variables of the clause (see Fig. 5). Within each clause gadget, we have a vertical (blue) stick b of length 2. Each horizontal (black) stick that bounds a clause gadget intersects a short vertical (black) stick of length ε to force b into its designated clause gadget. Moreover, b is not isolated because it intersects a short (violet) stick of length ε .

Clearly, if Φ is satisfiable, there is a stick realization of the $\text{STICK}_A^{\text{fix}}$ instance obtained from Φ by our reduction by placing the sticks as described before (see also Fig. 6). In particular, the blue sticks can be placed as depicted in Fig. 5.



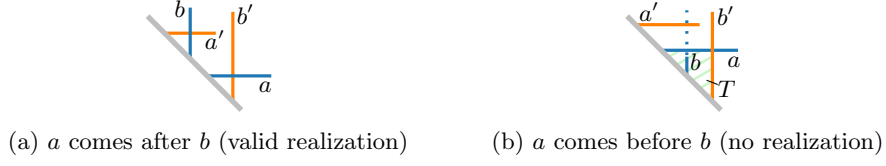


Fig. 7: Trying to realize a subgraph of the edges ab' and $a'b$ while respecting σ_A and σ_B .

On the other hand, if there is a stick realization of the $\text{STICK}_A^{\text{fix}}$ instance obtained by our reduction, Φ is satisfiable. As argued before, the shape of the (black) frame structure of all gadgets is fixed by the choice of the adjacencies and lengths in the graph and σ_A . The only flexibility is, for each $i \in \{1, \dots, n\}$, whether g_i has its foot point above or below r_i . This enforces one of eight distinct configurations per clause gadget. As depicted in Fig. 5, precisely the configurations that correspond to satisfying truth assignments are realizable. Thus, we can read a satisfying truth assignment of Φ from the variable gadgets. \square

We enforce an order of the horizontal sticks except for a set W of sticks, which are the short (violet) sticks of length ε that are adjacent to the red and the blue sticks in the variable and clause gadgets. For STICK_{AB} we can prescribe σ_B if we remove the sticks W and use the same reduction to obtain Corollary 2. Observe that we now have isolated vertices (the red and blue vertical sticks).

Corollary 2. $\text{STICK}_{AB}^{\text{fix}}$ with isolated vertices in A or B is NP-complete.

3.3 $\text{STICK}_{AB}^{\text{fix}}$ without isolated vertices

In this section, we constructively show that $\text{STICK}^{\text{fix}}$ is efficiently solvable if we are given a total order of the vertices in $A \cup B$ on the ground line. Note that if there is a realization for an instance of STICK_{AB} (and consequently also $\text{STICK}_{AB}^{\text{fix}}$), the combinatorial order of the sticks on the ground line is always the same except for isolated vertices, which we formalize in the following lemma.

Lemma 1. *In all realizations of an instance of STICK_{AB} , the order of the vertices $A \cup B$ on the ground line is the same after removing all vertices of degree 0. This order can be found in time $O(|E|)$.*

Proof. Assume there are realizations Γ_1 and Γ_2 of the same instance of STICK_{AB} without isolated vertices that have different combinatorial arrangements on the ground line. Without loss of generality, there is an $a \in A$ and a $b \in B$, such that in Γ_1 , a comes after b , while in Γ_2 , a comes before b (see Fig. 7). Clearly, a and b cannot be adjacent. Since a is not isolated, there is a b' that is adjacent to a and comes after b . Analogously, there is an a' that is adjacent to b and comes before a . In Γ_2 , a and b' define a triangle T (see Fig. 7b), which completely contains b since b occurs between a and b' , but is adjacent to neither of them. However, a' is outside of T as it comes before a . This contradicts b and a' being adjacent. The unique order can be determined in $O(|E|)$ time as described in Section 2. \square

We are given an instance of $\text{STICK}^{\text{fix}}$ and a total order v_1, \dots, v_n of the vertices ($n = |A| + |B|$) with stick lengths ℓ_1, \dots, ℓ_n . We create a system of difference constraints, that is, a linear program $Ax \leq b$ where each constraint is a simple linear inequality of the form $x_j - x_i \leq b_k$, with n variables and $m \leq 3n - 1$ constraints. Such a system can be modeled as a weighted graph with a vertex per variable x_i and a directed edge (x_i, x_j) with weight b_k per constraint. The system is solvable if and only if there is no directed cycle of negative weights, and a solution can be found in $O(nm)$ time with the Bellman-Ford algorithm.

For each stick v_i , we create a variable x_i that corresponds to the x-coordinate of v_i 's foot point on the ground line, with $x_1 = 0$. To ensure the unique order, we add $n - 1$ constraints $x_{i+1} - x_i \leq -\varepsilon$ for some suitably small ε and $i = 1, \dots, n - 1$.

Let $v_i \in A$ and $v_j \in B$. If $(v_i, v_j) \in E$, then the corresponding sticks have to intersect, which they do if and only if $x_j - x_i \leq \min\{\ell_i, \ell_j\}$. If $i < j$ and $(v_i, v_j) \notin E$, then the corresponding sticks must not intersect, so we require $x_j - x_i > \min\{\ell_i, \ell_j\} \geq \min\{\ell_i, \ell_j\} + \varepsilon$. This easily gives a system of difference constraints with $O(n^2)$ constraints. We argue that a linear number suffices.

Let $v_i \in A$. Let j be the largest j such that $(v_i, v_j) \in E$ and $\ell_j \geq \ell_i$. We add a constraint $x_j - x_i \leq \ell_i$. Further, let k be the smallest k such that $(v_i, v_k) \notin E$ and $\ell_k \geq \ell_i$. We add a constraint $x_k - x_i > \ell_i \Leftrightarrow x_i - x_k \leq -\ell_i - \varepsilon$. Symmetrically, let $v_i \in B$. Let j be the smallest j such that $(v_j, v_i) \in E$ and $\ell_j > \ell_i$. We add a constraint $x_i - x_j \leq \ell_i$. Further, let k be the largest k such that $(v_k, v_i) \notin E$ and $\ell_k > \ell_i$. We add a constraint $x_i - x_k > \ell_i \Leftrightarrow x_k - x_i \leq -\ell_i - \varepsilon$.

We now argue that these constraints are sufficient to ensure that G is represented by a solution of the system. Let $v_i \in A$ and $v_j \in B$. If $i > j$, then the corresponding sticks cannot intersect, which is ensured by the fixed order. So assume that $i < j$. If $\ell_j \geq \ell_i$ and $(v_i, v_j) \in E$, then we either have the constraint $x_j - x_i \leq \ell_i$, or we have a constraint $x_k - x_i \leq \ell_i$ with $i < j < k$; together with the order constraints, this ensure that $x_j - x_i \leq x_k - x_i \leq \ell_i$. If $\ell_j \geq \ell_i$ and $(v_i, v_j) \notin E$, then we either have the constraint $x_i - x_j \leq -\ell_i - \varepsilon$, or we have a constraint $x_i - x_k \leq -\ell_i - \varepsilon$ with $i < k < j$; together with the order constraints, this ensure that $x_i - x_j \leq x_i - x_k \leq -\ell_i - \varepsilon$. Symmetrically, the constraints are also sufficient for $\ell_j < \ell_i$. We obtain a system of difference constraints with n variables and at most $3n - 1$ constraints proving Theorem 5. By Lemma 1, there is at most one realizable order of vertices for a $\text{STICK}_{\text{AB}}^{\text{fix}}$ instance without isolated vertices, which can be found in linear time and proves Corollary 3.

Theorem 5. *$\text{STICK}^{\text{fix}}$ can be solved in $O((|A| + |B|)^2)$ time if we are given a total order of the vertices.*

Corollary 3. *$\text{STICK}_{\text{AB}}^{\text{fix}}$ without isolated vertices is solvable in $O((|A| + |B|)^2)$ time.*

4 Open Problems

We have shown that $\text{STICK}^{\text{fix}}$ is NP-complete even if the sticks have only three different lengths, while $\text{STICK}^{\text{fix}}$ for unit-length sticks is solvable in linear time. But what is the computational complexity of $\text{STICK}^{\text{fix}}$ for sticks with one of *two* lengths? Beside this, the complexity of the original problem STICK is still open.

References

1. Sergio Cabello and Miha Ježič. Refining the hierarchies of classes of geometric intersection graphs. *Electr. J. Comb.*, 24(1):P1.33, 2017. URL: <http://www.combinatorics.org/ojs/index.php/eljc/article/view/v24i1p33>.
2. Jean Cardinal, Stefan Felsner, Tillmann Miltzow, Casey Tompkins, and Birgit Vogtenhuber. Intersection graphs of rays and grounded segments. *J. Graph Algorithms Appl.*, 22(2):273–295, 2018. doi:10.7155/jgaa.00470.
3. Daniele Catanzaro, Steven Chaplick, Stefan Felsner, Bjarni V. Halldórsson, Magnús M. Halldórsson, Thomas Hixon, and Juraj Stacho. Max point-tolerance graphs. *Discrete Appl. Math.*, 216:84–97, 2017.
4. Jérémie Chalopin and Daniel Gonçalves. Every planar graph is the intersection graph of segments in the plane: Extended abstract. In *Proc. STOC*, pages 631–638. ACM, 2009. doi:10.1145/1536414.1536500.
5. Steven Chaplick, Paul Dorbec, Jan Kratochvíl, Mickaël Montassier, and Juraj Stacho. Contact representations of planar graphs: Extending a partial representation is hard. In *WG*, volume 8747 of *Lecture Notes Comput. Sci.*, pages 139–151. Springer, 2014.
6. Steven Chaplick, Stefan Felsner, Udo Hoffmann, and Veit Wiechert. Grid intersection graphs and order dimension. *Order*, 35(2):363–391, 2018. doi:10.1007/s11083-017-9437-0.
7. Steven Chaplick, Pavol Hell, Yota Otachi, Toshiki Saitoh, and Ryuhei Uehara. Ferrers dimension of grid intersection graphs. *Discrete Appl. Math.*, 216:130–135, 2017. doi:10.1016/j.dam.2015.05.035.
8. Stefan Felsner, Kolja B. Knauer, George B. Mertzios, and Torsten Ueckerdt. Intersection graphs of L-shapes and segments in the plane. In *MFCS (2)*, volume 8635 of *Lecture Notes Comput. Sci.*, pages 299–310. Springer, 2014. Some results herein are incomplete, see the warning on the full version: <http://page.math.tu-berlin.de/~felsner/Paper/dorgs.pdf>.
9. M. R. Garey and David S. Johnson. *Computers and Intractability: A Guide to the Theory of NP-Completeness*. W. H. Freeman, 1979.
10. Bjarni V. Halldórsson, Derek Aguiar, Ryan Tarpine, and Sorin Istrail. The clark phaseable sample size problem: Long-range phasing and loss of heterozygosity in GWAS. *Journal of Computational Biology*, 18(3):323–333, 2011.
11. Irith Ben-Arroyo Hartman, Ilan Newman, and Ran Ziv. On grid intersection graphs. *Discrete Math.*, 87(1):41–52, 1991. doi:10.1016/0012-365X(91)90069-E.
12. Michael Jünger, Sebastian Leipert, and Petra Mutzel. Level planarity testing in linear time. In *Graph Drawing*, volume 1547 of *Lecture Notes Comput. Sci.*, pages 224–237. Springer, 1998.
13. Pavel Klavík, Yota Otachi, and Jirí Sejnoha. On the classes of interval graphs of limited nesting and count of lengths. *Algorithmica*, 81(4):1490–1511, 2019.
14. Johannes Köbler, Sebastian Kuhnert, and Osamu Watanabe. Interval graph representation with given interval and intersection lengths. *J. Discrete Algorithms*, 34:108–117, 2015.
15. Jan Kratochvíl. A special planar satisfiability problem and a consequence of its NP-completeness. *Discrete Appl. Math.*, 52(3):233–252, 1994. doi:10.1016/0166-218X(94)90143-0.
16. Jan Kratochvíl and Jirí Matoušek. Intersection graphs of segments. *J. Comb. Theory, Ser. B*, 62(2):289–315, 1994.

17. Dieter Kratsch, Ross M. McConnell, Kurt Mehlhorn, and Jeremy P. Spinrad. Certifying algorithms for recognizing interval graphs and permutation graphs. *SIAM J. Comput.*, 36(2):326–353, 2006.
18. Wing Ning Li. Two-segmented channel routing is strong NP-complete. *Discrete Applied Mathematics*, 78(1-3):291–298, 1997. doi:10.1016/S0166-218X(97)00020-6.
19. Felice De Luca, Md. Iqbal Hossain, Stephen G. Kobourov, Anna Lubiw, and Debajyoti Mondal. Recognition and drawing of stick graphs. In Therese C. Biedl and Andreas Kerren, editors, *Proc. 26th Int. Symp. Graph Drawing & Network Vis.*, volume 11282 of *Lecture Notes Comput. Sci.*, pages 303–316. Springer, 2018. doi:10.1007/978-3-030-04414-5_21.
20. Jiří Matoušek. Intersection graphs of segments and $\exists\mathbb{R}$. ArXiv, <https://arxiv.org/abs/1406.2636>, 2014.
21. Itsik Pe’er and Ron Shamir. Realizing interval graphs with size and distance constraints. *SIAM J. Discrete Math.*, 10(4):662–687, 1997.
22. Marcus Schaefer. Complexity of some geometric and topological problems. In *Graph Drawing*, volume 5849 of *Lecture Notes Comput. Sci.*, pages 334–344. Springer, 2009. doi:10.1007/978-3-642-11805-0_32.
23. Malay K. Sen and Barun K. Sanyal. Indifference digraphs: A generalization of indifference graphs and semiorders. *SIAM J. Discrete Math.*, 7(2):157–165, 1994. doi:10.1137/S0895480190177145.
24. Anish Man Singh Shrestha, Asahi Takaoka, Satoshi Tayu, and Shuichi Ueno. On two problems of nano-pla design. *IEICE Transactions*, 94-D(1):35–41, 2011.
25. Jeremy Spinrad, Andreas Brandst dt, and Lorna Stewart. Bipartite permutation graphs. *Discrete Appl. Math.*, 18(3):279–292, 1987. doi:10.1016/S0166-218X(87)80003-3.

Appendix

A Omitted proofs of Section 2

Theorem 1. *STICK_A can be solved in $O(|A||B|)$ time.*

Proof (Continued). We continue the proof by first noting how one can handle disconnected graphs, and then discussing the backtracking and representation construction.

To handle disconnected graphs, we first identify the connected components H_1, \dots, H_t of G . We label each element of A by the index of the component to which it belongs. Now, observe that if σ_A contains a pattern of indices that alternate *abab*, then there can be no solution to STICK_A. Otherwise, we can treat each component separately by our algorithm, and then nest the resulting representations (whose construction we describe next via the backtracking) according to how the components nest in σ_A .

It remains to show how to do the backtracking and how to obtain the running time. The size of each data structure \mathcal{T}^p is in $O(|B^p|)$, since there are no degree-2 vertices in the trees and each leaf corresponds to a vertex in B . In each event, the transformations can clearly be done in time proportional to the size of the data structures. Since $|B^p| \leq B$ for each p and there are $2|A|$ events, the whole construction works in $O(|A||B|)$ time.

In the main text, we said that whenever a node x has exactly one child y and that child is an internal node, we merge x with its parent z . Instead of doing this, we will create a “shortcut” from y to z (and associate this shortcut with the last operation which caused x to be in this state). This way, we can traverse the tree without having to look at internal degree-2 nodes, but we keep them in the data structure for future reference. Also, we do not remove any leaves from the tree; we just mark them as *dead* and do not consider them anymore.

Assume that the algorithm processes all events without stopping. This means that, in every step, there was some realizable permutation. We now consider the data structure $\mathcal{T}^{|A| \mapsto}$. Since we never actually removed anything but just marked leaves as dead and introduced shortcuts, removing the shortcuts and marking leaves as alive can be done in $O(|A||B|)$ time. This gives us a data structure \mathcal{T} that contains all vertices of B as leaves. In particular, \mathcal{T} gives us a permutation σ_B of B . Moreover, for every event p , σ_B restricted to B^p is a realizable permutation of B^p due to G^p . Thus, executing our algorithm for STICK_{AB} on σ_A and σ_B gives us a stick representation of G . \square

B Omitted proofs of Section 3

We modify the reduction used in the proof of Theorem 3 so that we use only three lengths. To this end, we use paths of sticks of length ε . We refer to them as ε -paths. Like a spring, an ε -path can be stretched (Fig. 8a) and compressed (Fig. 8c) up to a specific length. We will exploit the following properties regarding the minimum and the maximum size of an ε -path.

Lemma 2. *There is a stick graph realization of a $2n$ -vertex ε -path with height and width $n\varepsilon$ and another realization with height and width $\frac{n+2}{3}\varepsilon + \delta$ for any $\delta > 0$ and $n \geq 3$. Any realization has height and width in the range $(\frac{n}{3}, n]\varepsilon$.*

Proof. We can arrange our sticks such that the foot points or the end points of two adjacent sticks touch each other (see Fig. 8a). This construction has height and width $n\varepsilon$ and, clearly, this is the maximum width and height for a $2n$ -vertex ε -path.

For the compressed ε -paths, we first describe a construction that has the specified width and height and, second, we show the lower bound.

The following construction is depicted in Fig. 8d for $n = 3$. Set the foot point of the first vertical stick in the path to $y = 0$ and the foot point of the third stick, which is also vertical, to $y = \varepsilon/3$. For each $i \in \{2, \dots, n-1\}$, set the foot point of the $(2i-2)$ -th stick (horizontal) to $y = i\varepsilon/3 + (i-2)\delta/(n-2)$ and the foot point of the $(2i+1)$ -th stick (vertical) to $y = i\varepsilon/3 + (i-1)\delta/(n-2)$. Set the foot point of the $(n-2)$ -th stick to $y = n\varepsilon/3 + \delta$, and the foot point of the last stick to $y = (n+1)\varepsilon/3 + \delta$. Observe that this construction has width and height $\frac{n+2}{3}\varepsilon + \delta$ and is a valid stick representation of a $2n$ -vertex ε -path.

Consider the i -th stick of an ε -path. On the one side of the line through this stick, there is the $(i-3)$ -th stick, and on the other, there is the $(i+3)$ -th stick. E.g., the second stick is to the right of the fifth stick and the eighth stick is to the left of the fifth stick. Since all sticks have length ε and non-adjacent sticks are not allowed to touch each other, the 1st, 4th, 7th, \dots , $(6k-2)$ -th stick for $k \in \mathbb{N}$ form a zigzag chain of width and height strictly greater than $k\varepsilon$. The same holds for the 2nd, 5th, \dots stick and the 3rd, 6th, \dots stick. Thus, for an ε -path of $2n$ sticks, we have width and height strictly greater than $\lceil \frac{2n}{6} \rceil \varepsilon \geq \frac{n}{3}\varepsilon$. \square

Corollary 1. *STICK^{fix} with only three different stick lengths is NP-complete.*

Proof. We modify the reduction from 3-PARTITION to STICK^{fix} described in the proof of Theorem 3 such that we use only three distinct stick lengths. We use the three lengths ε , Cm , and $3Cm$ (or longer, e.g. ∞). In Fig. 9, sticks of these lengths are violet, black, and green, respectively.

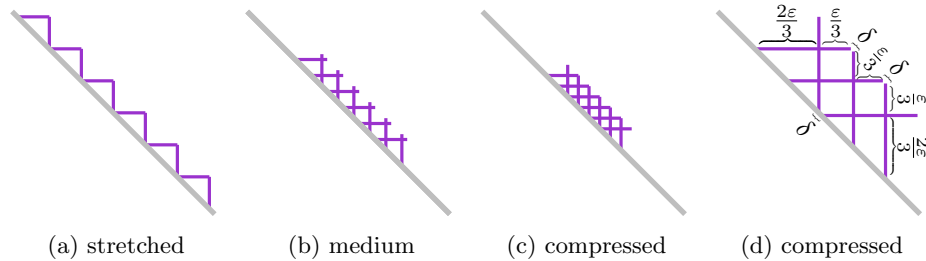


Fig. 8: An ε -path of 12 sticks in (a)–(c) and 6 sticks in (d).

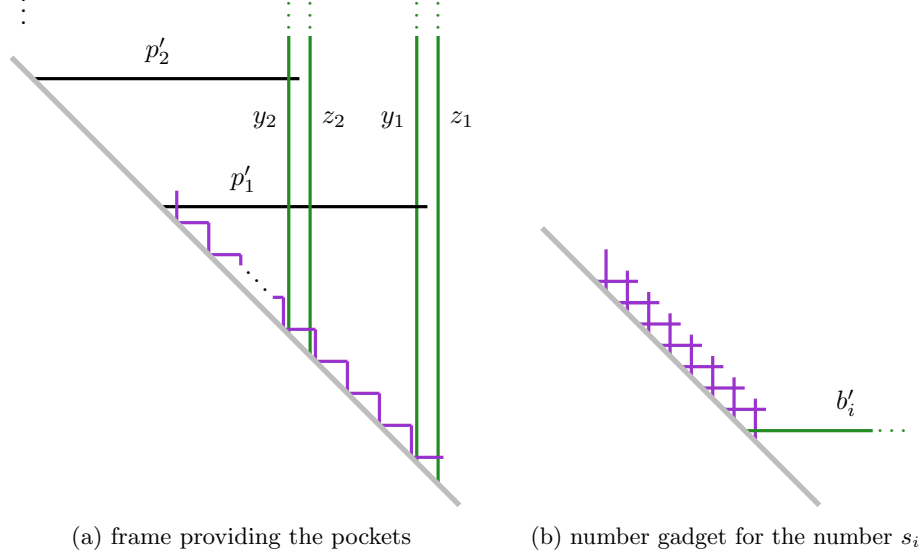


Fig. 9: Gadgets of our reduction from 3-PARTITION to $\text{STICK}^{\text{fix}}$ with three stick lengths.

First, we describe the modifications of the frame structure, which are also depicted in Fig. 9a. Instead of the vertical (green) sticks x , y , and z used to fix all pockets, we have two vertical sticks y_j and z_j of length $3Cm$ for $j \in \{1, \dots, m+1\}$. Instead of the sticks p_1, \dots, p_{m+1} of different lengths, we use horizontal (black) sticks p'_1, \dots, p'_{m+1} each with length Cm to separate the pockets. The stick p'_j intersects y_k, z_k for all $k \in \{j+1, \dots, m+1\}$ and y_j but not z_j . All pairs y_j-z_j are kept together by a stick of length ε . For each two neighboring pairs y_j-z_j and $y_{j+1}-z_{j+1}$, these sticks of length ε are connected by an ε -path of $2C/\varepsilon$ sticks. According to Lemma 2, this effects a maximum distance of $(C/\varepsilon) \cdot \varepsilon \pm \varepsilon = C \pm \varepsilon$ between each two pairs of y_j-z_j and $y_{j+1}-z_{j+1}$. Accordingly, the pockets separated by the sticks p'_1, \dots, p'_{m+1} have height at most $C \pm 2\varepsilon$, similar as in the proof of Theorem 3. We keep the vertical (orange) stick o as in Figure 3a to prevent number gadgets from being placed above the topmost pocket, but now o has length $3Cm$.

Second, we describe the modifications of the number gadgets for each number s_i for $i \in \{1, \dots, 3m\}$, which are also depicted in Fig. 9b. We keep a long stick b'_i similar to b_i —now with length $3Cm$. We replace r_i (and h_i and v_i) by an ε -path of $6s_i/\varepsilon - 4$ sticks. We make the first stick of the ε -path intersect b'_i . By Lemma 2, this ε -path can be realized with height $s_i + \delta$ for any $\delta > 0$, but there is no realization with height $s_i - \frac{2}{3}\varepsilon$ or smaller. Clearly, these number gadgets can only be placed into one pocket since none of their sticks intersects a p'_j for $j \in \{1, \dots, m+1\}$.

Hence, we can represent a yes-instance of 3-PARTITION as such a stick graph if and only if the ε -paths of the number gadgets are (almost) as much compressed

as possible (to make the number gadgets small enough) and the ε -paths between the y_j - z_j sticks are (almost) as much stretched as possible (to make the pockets tall enough). Using this, the proof is the same as in Theorem 3. \square